

# WAVEFUNCTION-ENGINEERING OF INTERSUBBAND THz-LASER NANOHETEROINTERFACES

EMMANUEL A. ANAGNOSTAKIS

*Hellenic Air Force Academy,  
Dekeleia, Attica, Greece  
emmanagn@otenet.gr*

(Received 10 December 2010; revised manuscript received 15 January 2011)

**Abstract:** A novel THz-luminescence laser nanoheterointerfacial scheme of the intersubband, longer-wavelength limit, mid-infrared functionality type has been designed on the basis of optically-pumped dual-resonant tunnelling of conductivity electrons within an appropriately energetically-determined configuration of five subbands hosted by two communicating asymmetric, approximately rectangular quantum wells (QWs).

The employed upper laser-action level is the second excited subband of the nanostructure back, wider QW and is provided with electrons via resonant tunnelling from the first excited subband of the nanostructure front QW populated through remotely ignited optical pumping out of the local fundamental subband.

On the other hand, the first excited back-QW subband functions as the lower laser action level, directly delivering the received electrons to the local fundamental subband via a fast vertical longitudinal optical phonon scattering. From there, they are recycled back to the nanostructure front QW fundamental subband by virtue of a second, reverse sense resonant-tunnelling-mediated normal charge transport mechanism.

A nanophotonics application of the scheme predicts laser operability in the 15-THz range.

**Keywords:** optoelectronic nanodevices, nanophotonics, THz-laser nanoheterointerfaces

## 1. Introduction

The investigation of semiconductor heterointerfaces is a prominent subject of ongoing research in view of their significance for the functionality of numerous optoelectronic microdevices [1–6]. For more than two decades, the designing strategy of wavefunction-engineering [7] has produced an admirable wealth of innovative semiconductor devices, characterized by a high degree of tunability in their optoelectronic performance. Celebrated pioneering microelectronic heterostructures of this kind are the Bloch oscillator [8, 9], the resonant tunnelling double heterodiode [10], the hot electron tunnelling transistor [11], and the revolutionary quantum cascade, laser [12, 13].

In the present paper, the principle of operation of an intersubband, far mid-infrared unipolar laser action heterostructure is outlined. It is based on optically pumped dual resonant tunnelling between two quantum wells (QWs), asymmetric both spatially and with respect to the height of the energy barrier. This is effected in terms of band-gap engineering and quantum mechanical conductivity vertical electron transport and local (within each QW) energetic transitions.

In Section 2, the required laser action level population inversion is monitored via a rate equation formalism against the ratio of crucial time constants characterising the two successive resonant tunnelling processes involved. Intervening intersubband longitudinal-optical-phonon scattering is also employed. In Section 3, a generic application of the operational principle to a model four-semiconductor nanostructure predictably emitting in the 20mm far mid-infrared coherent electromagnetic radiation spectrum band is discussed. A measure of the optoelectronic yield of the designed nanodevice is given by the intersubband stimulated optical gain, through the laser action population inversion, in terms of the subband lifetimes entailed.

## 2. THz-laser action: wavefunction-engineering

This paper proposes a novel operation principle for a laser action nano-heterostructure [14], based on remotely optically pumped [15, 16] dual resonant tunnelling (OPRT) unipolar charge transport mechanism which can be carried out within the framework of two communicating quantum wells (CQWs), asymmetric *both* spatially and with respect to their energy barrier height. The CQWs host a total of five partially-localised subbands, two of which (the fundamental  $I_f >$  and the first excited  $I_f' >$ ) are on the part of the envisaged device front ([F]) QW and the remaining three (the fundamental  $I_b >$ , the first excited  $I_b' >$ , and the second excited  $I_b'' >$ ) on the other part of the OPRT device back ([B]) QW. The aim of the band-gap-engineering design has been to establish – by means of a respective growth procedure – two selective energy matchings; one between the uppermost subbands  $I_f' >$  and  $I_b'' >$  of the two CQWs, and the other between the innermost fundamental sublevels  $I_f >$  and  $I_b >$  in the two neighbouring QWs (Figure 1).

The two laser-action levels of the OPRT nanodevice have been designed to correspond to the second excited  $I_b'' >$  [B] QW subband and the local next lower first excited  $I_b' >$  subband:

The upper OPRT laser action level is predicted to be continuously provided with conductivity electrons, resonantly tunnelling [17, 18] into it, from its energetically matched device front [F] QW first excited  $I_f' >$  subband. The latter would be populated through remotely ignited optical intersubband pumping from its local fundamental  $I_f >$  front QW subband. The lower OPRT nanostructure laser action level, on the other hand, is expected to be directly delivering its radiatively de-excited electrons to the local device back [B] QW fundamental  $I_b >$  subband via particularly fast longitudinal optical (LO) phonon scattering. This LO phonon

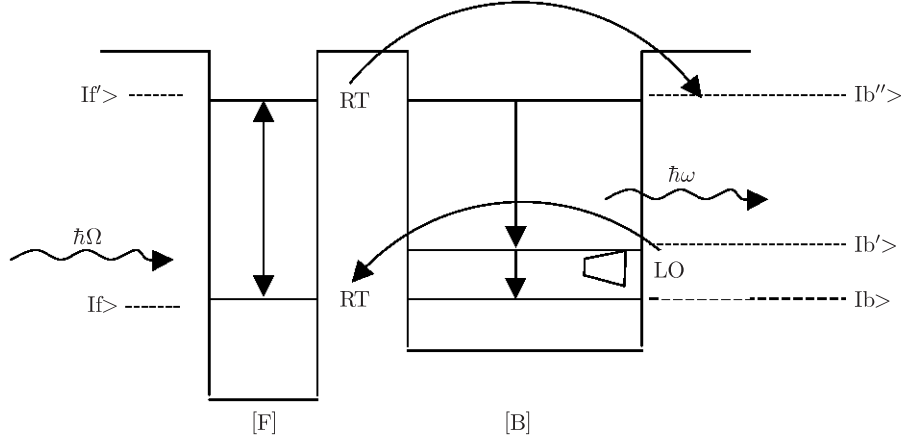


Figure 1. Wavefunction-engineering of the proposed THz-laser

scattering is almost vertical in the reciprocal space and favoured by a band-gap-engineered energetic proximity of the entailed  $Ib'> \leftrightarrow Ib>$  intersubband separation with the characteristic LO phonon energy valid under the operational conditions within the [B] QW semiconductor material.

Furthermore, the considered functionality of the OPRT laser nanostructure resonant microcavity [19, 20] is determined by the above-mentioned LO phonon scattering of radiatively down-converted conductivity electrons (from the laser action lower level to the local [B] QW fundamental subband) and by their being recycled back to the OPRT laser nanostructure [F] QW fundamental  $If>$  subband by virtue of a second, reverse sense, resonant-tunnelling-mediated normal charge transport mechanism.

The rate equations modelling the laser action functionality of the subband levels  $Ib''>$  and  $Ib'>$  take the form:

$$\frac{dN_{Ib''>}}{dt} = \frac{1}{T_{FB}} N_{If'>} - \frac{1}{\tau_{Ib''>}} N_{Ib''>} \quad (1)$$

$$\frac{dN_{Ib'>}}{dt} = \frac{1}{\tau} N_{Ib''>} - \frac{1}{\tau_{Ib'>}} N_{Ib'>} \quad (2)$$

where  $N_{If'>}$ ,  $N_{Ib'>}$  and  $N_{Ib''>}$  are the sheet electron concentrations of nanostructure resonator levels  $If'>$ ,  $Ib'>$  and  $Ib''>$ , respectively,  $\frac{1}{T_{FB}}$  is the temporal rate of achieving the resonant-tunnelling charge transport from the [F] QW first excited subband  $If'>$  onto the energetically commensurate [B] QW second excited subband  $Ib''>$ ,  $\tau_{Ib''>}$  is the total lifetime of the upper laser action level  $Ib''>$ , expressed by means of the  $Ib''> \rightarrow Ib'>$  combined radiative and non-radiative down-conversion rate ( $\frac{1}{\tau}$ ) and the  $Ib''> \rightarrow Ib>$  non-radiative direct relaxation rate ( $\frac{1}{\tau_{Ib''> \rightarrow Ib>}}$ ) as:

$$\frac{1}{\tau_{Ib''>}} = \frac{1}{\tau} + \frac{1}{\tau_{Ib''> \rightarrow Ib>}} \quad (3)$$

and  $\frac{1}{\tau_{Ib'>}}$  is the non-radiative fast vertical longitudinal optical phonon scattering rate of electrons received by the lower laser-action subband  $Ib'>$  to the local [B] QW fundamental subband  $Ib>$ .

Equations (1) and (2) form a system with five unknowns, namely  $N_{Ic>}$  ( $c = f, f', b, b', b''$ ), which are the areal electron densities of the five nanostructure resonator levels  $Ic>$ , along with the following equations:

$$\frac{dN_{If>}}{dt} = \frac{1}{T_{BF}} N_{Ib>} - \frac{I\Sigma}{\hbar\Omega} N_{If>} \quad (4)$$

$$\frac{dN_{If'>}}{dt} = \frac{I\Sigma}{\hbar\Omega} N_{If>} - \frac{1}{T_{FB}} N_{If'>} \quad (5)$$

$$\frac{dN_{Ib>}}{dt} = \frac{1}{\tau_{Ib''>\rightarrow Ib>}} N_{Ib''>} + \frac{1}{\tau_{Ib'>}} N_{Ib'>} - \frac{1}{T_{BF}} N_{Ib>} \quad (6)$$

where  $\frac{1}{T_{BF}}$  denotes the temporal rate at which the (reverse sense)  $Ib>\rightarrow If>$  resonant electron-tunnelling is effected within the CQWs,  $I$  is the optical pumping intensity,  $\Omega$  is the pumping photon cyclic frequency, and  $\Sigma$  is the optical absorption cross section exhibited by the electrons initially resting upon the [F] QW fundamental subband level  $If>$  to incoming pumping photons.

On the other hand, the stimulated optical yield  $Y$  can be determined as [15]:

$$Y = \frac{1}{L} \sigma \Delta N \quad (7)$$

where  $L$  is the spatial extent of the entire CQWs configuration,  $\sigma$  is the laser-stimulated emission cross section for producing the secondary coherent photons (of energy  $\hbar\omega = \Delta E_{Ib''>\rightarrow Ib'>} = \Delta E$ );  $\Delta N$  is the laser action population inversion between the levels,  $Ib''>$  and  $Ib'>$  obtained from the above-mentioned rate equation system describing the electron concentration. This system can be solved at the steady state of the set of the different charge transport mechanisms within the OPRT nanoheterostructure.

The aforementioned model formalism, based on the monitoring of the rate equations of the proposed OPRT laser-action level-population evolution and inversion, incorporates the determination of the transmission coefficient [14, 17] for the consecutive steps of the resonant-tunnelling inter-QW communication mechanism.

### 3. Application of OPRT laser: functionality and discussion

In order to carry out the proposed scheme, we consider an indicative generic semiconductor nanoheterostructure based on the conventional  $Al_xGa_{1-x}As/GaAs$  system.

In particular, we employ two quantum wells which are asymmetric both spatially and with respect to the energy barrier height. The quantum wells are approximately rectangular and communicate through an intervening barrier layer. Both wells are formulated within (different portions of) the GaAs semiconductor: The front QW [F] with a spatial width of 96Å and an energy barrier height

of 221 meV is contained between a surface  $\text{Al}_{0.3}\text{Ga}_{0.7}\text{As}$  slab and an inter-QW communication barrier layer. The back QW [B] with an extension of 162 Å and an energetic confinement hill of 204 meV, spans the region between the inter-QW communication barrier layer and a bottom  $\text{Al}_{0.33}\text{Ga}_{0.67}\text{As}$  slab. The intervening communication barrier layer may be regarded as a succession of two similar-thickness sublayers of  $\text{Al}_{0.3}\text{Ga}_{0.7}\text{As}$  and  $\text{Al}_{0.33}\text{Ga}_{0.67}\text{As}$ .

We then proceed with algorithmic [21] calculations, which transform the pertinent Schrödinger equation (concerning the electron de Broglie time-independent wavefunction and taking into account the spatial variation of the carrier effective mass) into a tridiagonal-matrix eigenvalue system (by rearranging it as the Sturm-Liouville case).

In this manner, the partially-localised conductivity-electron eigenstates, accommodated by the two communicating QWs in the model application under study, correspond to the energy eigenvalues (measured within each QW, going upwards from its energetic bottom):  $E(\text{If}) = 32\text{ meV}$ ,  $E(\text{If}') = 136\text{ meV}$  for the front QW fundamental and first excited bound state, respectively; and  $E(\text{Ib}) = 14\text{ meV}$ ,  $E(\text{Ib}') = 55\text{ meV}$ , and  $E(\text{Ib}'') = 121\text{ meV}$  for the back QW fundamental, first- and second-excited bound state, respectively.

Notably, the fundamental eigenstates of the two CQWs are well aligned, given that their intra-QW heights differ by almost the inter-QW bottom-asymmetry.

In an analogous manner, the uppermost bound eigenstates of the two communicating QWs emerge aligned, since the difference between their intra-QW heights almost cancels the energetic height asymmetry of the two QW bottoms.

The ensuing calculations involve the determination of the effective dipole lengths, which are associated with the intersubband transitions, collaborating with, or antagonising one another through the nanooptoelectronic structure. The intersubband transition-lifetime engineering thus becomes equivalent to the original wavefunction-engineering attempted. Furthermore, the determined intersubband transition (ISBT) effective dipole lengths demonstrate the oscillator strengths supporting the different ISBT events, whereas the predicted laser-action population-inversion leads to the device-stimulated optical gain.

Results (radiative transition time constant around 45 ns, corresponding to an ISBT dipole length  $\langle b''|z|b' \rangle$  of about 1 nm), are connected with a laser far mid-infrared emission OPRT functionality in the range of 65 meV/15 THz, with a stimulated optical gain  $Y$  sensitivity  $\frac{\partial Y}{\partial I}$  to the pumping illumination power  $I$  around  $11 \frac{\text{cm}^{-1}}{10^5 \text{ W/cm}^2}$ .

## References

- [1] Harris J J, Murray R and Foxon C T 1993 *Semicond. Sci. Technol.* **8** 31
- [2] Li Shengs S, Chuang M Y and Yu L S 1993 *Semicond. Sci. Technol.* **8** 406
- [3] Logansen L V, Malov V V and Xu J M 1993 *Semicond. Sci. Technol.* **8** 568
- [4] Juang C 1991 *Phys. Rev. B* **44** 10706
- [5] Asbel M Ya 1992 *Phys. Rev. Lett.* **68** 98

- [6] Papadopoulos G J 1997 *J. Phys. A.* **30** 5497
- [7] Capasso F and Cho A Y 1994 *Surf. Sci.* **299/300** 878
- [8] Grondin R O, Porod W, Ho J, Ferry D K and Iafrate G J 1985 *Superlattices and Microstructures* **1** 183
- [9] Churchill J N and Holmstrom F E 1981 *Phys. Lett. A* **85** 453
- [10] Sollner T C L G, Goodhue W D, Tannenwald P E, Parker C D and Peck D D 1983 *Appl. Phys. Lett.* **43** 588
- [11] Yokoyama N, Imamura K, Oshima T, Nishi H, Muto S, Kondo K and Hiyamizu S 1984 *J. Appl. Phys.* **23** L311
- [12] Faist J, Capasso F, Sivco D, Sirtori D, Hutchinson A L, Chu S N G and Cho A Y 1994 *Science* **264** 553
- [13] Faist J, Capasso F, Sirtori C, Sivco D L, Hutchinson A L and Cho A Y 1996 *Electron. Lett.* **32** 560
- [14] Singh J 1995 *Semiconductor Optoelectronics* Chap. 10, McGraw-Hill, New York
- [15] Julien G H, Gauthier-Lafaye O, Boucaud P, Sauvage S, Lourtioz J-M, Thierry-Mieg V and Phanel R 1998 *Intersubband Transitions in Quantum Wells: Physics and Devices* Chap. 1, Kluwer Academic Publishers, Boston
- [16] Anagnostakis E A 1994 *Phys. Stat. Sol. B* **181** K15
- [17] Bastard G 1987 *Wave Mechanics Applied to Semiconductor Heterostructures* Chap. IV, VI, Les Edition de Physique, Les Ulis Cedex, France
- [18] Chiou W-H, Pan H-J, Liu R-Ch, Chen Ch-Y, Wang Ch-K, Chuang H-M and Liu W-Ch 2002 *Semicond. Sci. Technol.* **17** 87
- [19] Pessa M, Guina M, Dumitrescu M, Hirvonen I, Saarinen M, Toikkanen L and Xiang N 2002 *Semicond. Sci. Technol.* **17** R1
- [20] Kulakovskii V D, Tartakovskii A I, Krizhanovskii D N, Gippius N A, Skolnick M S and Roberts J S 2001 *Nanotechnology* **12** 475
- [21] Anagnostakis E A 2008 *J. Non-Cryst. Sol.* **354** 4233